Science of the Total Environment 408 (2010) 3277–3291

Contents lists available at ScienceDirect

Science of the Total Environment

journal homepage: www.elsevier.com/locate/scitotenv

Study of atmospheric mercury budget in East Asia using STEM-Hg modeling system

Li Pan [a,*], Che-Jen Lin [a,b], Gregory R. Carmichael [c], David G. Streets [d], Youhua Tang [e], Jung-Hun Woo [f], Suraj K. Shetty [h], Hsing-Wei Chu [g], Thomas C. Ho [h], Hans R. Friedli [i], Xinbin Feng [j]

[a] Department of Civil Engineering, Lamar University, Beaumont, TX 77710, USA
[b] School of Environmental Science & Engineering, South China University of Technology, Guangzhou, 510006, Guangdong, China
[c] Center for Global and Regional Environmental Research at University of Iowa, Iowa City, IA 52242, USA
[d] Argonne National Laboratory, DIS/900, 9700 South Cass Avenue, Argonne, IL 60439, USA
[e] NOAA/NWS/NCEP/EMC, 5200 Auth Road WWB #207, Camp Springs, MD 20746, USA
[f] Department of Advanced Technology Fusion, 1 Hwayang-dong, Gwangjin-Gu, Seoul Korea, Seoul, Seoul 143-701, South Korea
[g] Department of Mechanical Engineering, Lamar University, Beaumont, TX 77710, USA
[h] Department of Chemical Engineering, Lamar University, Beaumont, TX 77710, USA
[i] National Center for Atmospheric Research, Boulder, CO 80307, USA
[j] State Key Laboratory of Environmental Geochemistry, Institute of Geochemistry, Chinese Academy of Sciences, Guiyang 550002, China

ARTICLE INFO

Article history:
Received 2 February 2010
Received in revised form 16 April 2010
Accepted 20 April 2010
Available online 21 May 2010

Keywords:
Mercury
Chemical transport
East Asia
Seasonal variation
Mass budget

ABSTRACT

East Asia is the largest source region of global anthropogenic mercury emissions, and contributes to atmospheric mercury concentration and deposition in other regions. Similarly, mercury from the global pool also plays a role in the chemical transport of mercury in East Asia. Annual simulations of atmospheric mercury in East Asia were performed using the STEM-Hg modeling system to study the mass budgets of mercury in the region. The model results showed strong seasonal variation in mercury concentration and deposition, with signals from large point sources. The annual mean concentrations for gaseous elemental mercury, reactive gaseous mercury and particulate mercury in central China and eastern coastal areas were 1.8 ng m^{-3}, 100 pg m^{-3} and 150 pg m^{-3}, respectively. Boundary conditions had a strong influence on the simulated mercury concentration and deposition, contributing to 80% of the concentration and 70% of the deposition predicted by the model. The rest was caused by the regional emissions before they were transported out of the model domain. Using different oxidation rates reported for the Hg^0–O_3 reaction (i.e., by Hall, 1995 vs. by Pal and Ariya, 2004) led to a 9% difference in the predicted mean concentration and a 40% difference in the predicted mean deposition. The estimated annual dry and wet deposition for East Asia in 2001 was in the range of 590–735 Mg and 482–696 Mg, respectively. The mercury mass outflow caused by the emissions in the domain was estimated to be 681–714 Mg yr^{-1}. This constituted 70% of the total mercury emission in the domain. The greatest outflow occurred in spring and early summer.

Published by Elsevier B.V.

1. Introduction

Mercury, a known potent neural toxin, can be transported over long distances from the source areas due to the long atmospheric lifetime (0.6–1.5 years) of gaseous elemental mercury (GEM) (Slemr et al., 1985; Pan and Carmichael, 2005). On the other hand, it can be quickly removed from the atmosphere via wet and dry deposition of its divalent oxidation state, either in the forms of reactive gaseous mercury (RGM) or particulate mercury (PHg). Its bio-accumulation in the food chain after deposition and methylation causes major concern for mercury pollution (Rolfhus et al., 2003).

East Asia is the largest mercury source region in the world. It contributes to about 40–50% of global mercury input to the atmosphere from anthropogenic sources (Pacyna et al., 2006). Circumpolar westerlies in the mid-latitude transport mercury plumes emitted in East Asia to North America. Such long-range transport contributes to mercury deposition in different regions of North America (Seigneur et al., 2004; Selin and Jacob, 2008; Strode et al., 2008). Being a global pollutant, mercury emissions from other source regions may also influence the air concentration and deposition of mercury in East Asia. However, few efforts have been made to address this issue. Preliminary measurements and modeling analyses have suggested that mercury outflow from the East Asian region may be significant (Friedli et al., 2004; Pan et al., 2006, 2007, 2008).

To assess how the mercury concentration and deposition can be influenced by the long-range transport either from East Asia to other regions or from other regions to East Asia, a better understanding of mercury transport, transformation and deposition in the East Asian region is necessary. In this study, the mercury extension of the Sulfur Transport Eulerian Model (STEM-Hg) was applied to simulate the

* Corresponding author.
E-mail address: lpan@my.lamar.edu (L. Pan).

0048-9697/$ – see front matter. Published by Elsevier B.V.
doi:10.1016/j.scitotenv.2010.04.039

mercury emission, transport and deposition in East Asia for model year 2001. The model results provided insights to the cycling of atmospheric mercury and its seasonal variability. In addition, the mass budgets of mercury were estimated from the model results to investigate the quantity of mercury outflows from the domain as well as the influence caused by the oxidation kinetics of Hg^0–O_3 reaction. The influences of boundary conditions and their implications on the chemical transport of atmospheric mercury in the regions were examined.

2. Methodology

2.1. Model descriptions

STEM-Hg is the mercury model of the Sulfur Transport and dEposition Model (STEM-III), developed at the University of Iowa. It is an Eulerian model that accounts for the transport, chemistry, and deposition of atmospheric pollutants in gaseous, aqueous and particulate phases (Carmichael et al., 1986, 1991, 1998, 2003; Tang et al., 2003).

Mercury reactions in both gaseous and aqueous phases are included in STEM-Hg. In the gas phase, GEM is oxidized to form PHg from the oxidation mediated by O_3 and OH; and to form RGM from the oxidation by chlorine. The subsequent partition of RGM and PHg into droplets contributes to the mercury concentrations in the aqueous phase where it undergoes redox ($Hg^0 \Leftrightarrow Hg^{2+}$) and equilibrium reactions. The mercury mechanism in the model was originally based on Lin and Pehkonen (Lin and Pehkonen, 1999). Other atmospheric reactions in the gas phase, such as photochemistry, are governed by SAPRC-99 mechanism (Carter, 2000). The model details and formulations have been reported in our earlier work (Pan and Carmichael, 2005; Pan et al., 2008).

The wet removal of RGM and PHg in STEM-Hg was treated similarly to that of nitric acid and sulfate aerosols, respectively. It was derived from the ATMOS model (Calori and Carmichael, 1999). The wet removal rate was calculated as a function of the precipitation rate, rainwater contents and cloud water contents. The vertical distributions of aqueous mercury concentration in the cloud water and in precipitation was also considered. Therefore, the wet deposition flux of Hg(II) in the aqueous phase can be expressed as:

$$F_{\text{wet}} = \sum_{k=1}^{\text{top}} K_{\text{w}}|_k \times \left[Hg_k^{2+}\right]_{\text{aq}}$$

where $[Hg_k^{2+}]_{\text{aq}}$ and $K_{\text{w}}|_k$ are the divalent mercury concentration and the wet removal velocity in the layer of k, respectively.

In this study, the GEM dry deposition velocity was set to zero assuming that its deposition flux can be balanced by the re-emission, similar to that applied in the NOAA HYSPLIT-Hg model. This assumption was shown to be able to satisfactorily explain ambient mercury concentrations (Bullock and Brehme, 2002; Cohen et al., 2004). The dry deposition velocity for RGM and PHg is calculated based on the parameterization of Wesely (1989) for gaseous HNO_3 and sulfate deposition velocity, respectively.

2.2. Emissions

Mercury emission inventories used in this study are summarized in Table 1. Mercury emission inventory in China was based on the work of Streets et al. (2005), reporting anthropogenic mercury emissions of 536 (±236) Mg annually in 1999. Averaging the contribution from all the source categories, the speciation profiles were 56% GEM, 32% RGM, and 12% PHg. The emission inventories outside China were based on the work of Pacyna et al. (2006), totaling 106 Mg of GEM, 62 Mg of RGM and 15 Mg of PHg. The total annual anthropogenic emissions within the domain are 406 Mg of GEM, 233 Mg of RGM and 79 Mg of PHg. The spatial distributions of mercury emissions are shown in Fig. 1. Mercury emissions in China were mainly from nonferrous metal smelting and coal combustion (Streets et al., 2005). The emissions in Japan and South Korea came mainly from waste incineration (Sakata and Marumoto, 2002). The natural emission in the domain was estimated to be 304 Mg year^{-1} (Pan et al., 2006), which were temporally allocated based on temperature and solar radiation similar to the work of Gbor et al. (2007). GEM emissions from biomass burning were calculated using CO emissions taken from climatological global estimates (Reddy and Boucher, 2004) and the GEM/CO ratio for biomass plumes observed during Ace-Asia (Friedli et al., 2004), which occurred mainly in March and April was estimated to be 27.7 Mg in 2001.

Table 1
Summary of mercury emissions used in the model simulations for the model year of 2001 (unit: Mg).

Regions	GEM		RGM		PHG	
Anthrop. China	Area	171	Area	112	Area	57
	Point	129	Point	59	Point	7
Anthrop. other countries[a]	Area	87	Area	56	Area	12
	Point	19	Point	6	Point	3
Natural	304		–		–	
Total	710		233		79	

[a] Indicates the anthropogenic emissions in the study domain excluding the emission in China.

Mercury anthropogenic emission in China used in the simulation was in the year of 1999 (Streets et al., 2005). Anthropogenic mercury emission in the domain region other than China was in the year of 2000 (Pacyna et al., 2006). Mercury emission from nature sources and re-emission was derived from the inventory in the year of 1999 (Pan et al., 2006). Wu et al. (2006) reported an averaged 2.9% increase in mercury emissions from anthropogenic sources in China from 1995 to 2003 (Wu et al., 2006). We recognized that the emission inventory year did not match the year of model simulation. However, the emission data were the best estimates available at the time when the modeling was conducted.

2.3. Model simulation

The East Asian model domain consists of 117 × 108 horizontal grids at 50 km spatial resolution with 17 vertical layers (up to 8 km) defined at the midpoint of sigma-z layers. The simulation period was for 12 months in 2001. The Penn State/NCAR Mesoscale model MM5 outputs (Grell, 1995) driven by the NCEP/NCAR global reanalysis were used to provide meteorological fields. The domain covers China and North and South Korea, southern Mongolia and part of Japan and Southeast Asia (Fig. 1a).

To understand how mercury emissions, boundary conditions, and oxidation kinetics of Hg^0 by O_3 influenced the model results, simulations for several model scenarios were performed. The base case simulation, denoted as "2001_BASE", used the boundary conditions extracted from a global 3-D chemical transport model (GEOS-Chem) (Selin et al., 2007) and a lower Hg^0–O_3 reaction rate (Hall, 1995). The chemistry set used in the GEOS-Chem model was essentially the same as STEM. For example, the rates of mercury gas phase reactions with O_3 and OH radical were the same and both models included mercury reduction in the aqueous phase. The spatial distributions of GEM obtained from GEOS-Chem simulations in East Asia (figure was not shown) were quite similar to those obtained from our STEM simulations, except that GEOS-Chem predicted higher values. This was primarily caused by the greater natural mercury emission in the GEOS-Chem simulations (Selin et al., 2007). We realized that the science inconsistencies between global and regional models in mercury chemical and physical mechanisms may be a

concern, but this was not the case in this study. This issue will be discussed in another manuscript.

Several other cases representing different emission scenarios, boundary conditions, and mercury oxidation chemistry were also performed. The case "2001_BASE_NOEM" assumed zero mercury emission in the domain for assessing the impact of mercury emission sources. The case "2001_CLEAN" assumed a "clean" atmospheric background concentration of mercury to investigate the importance of boundary conditions. The "clean" background was defined as 1.2 ng m^{-3} of GEM and zero RGM and PHg in both initial and boundary conditions. The 1.2 ng m^{-3} as a clean background concentration of GEM was based on ACE-Asia mercury observation data, in which we defined mercury background concentration

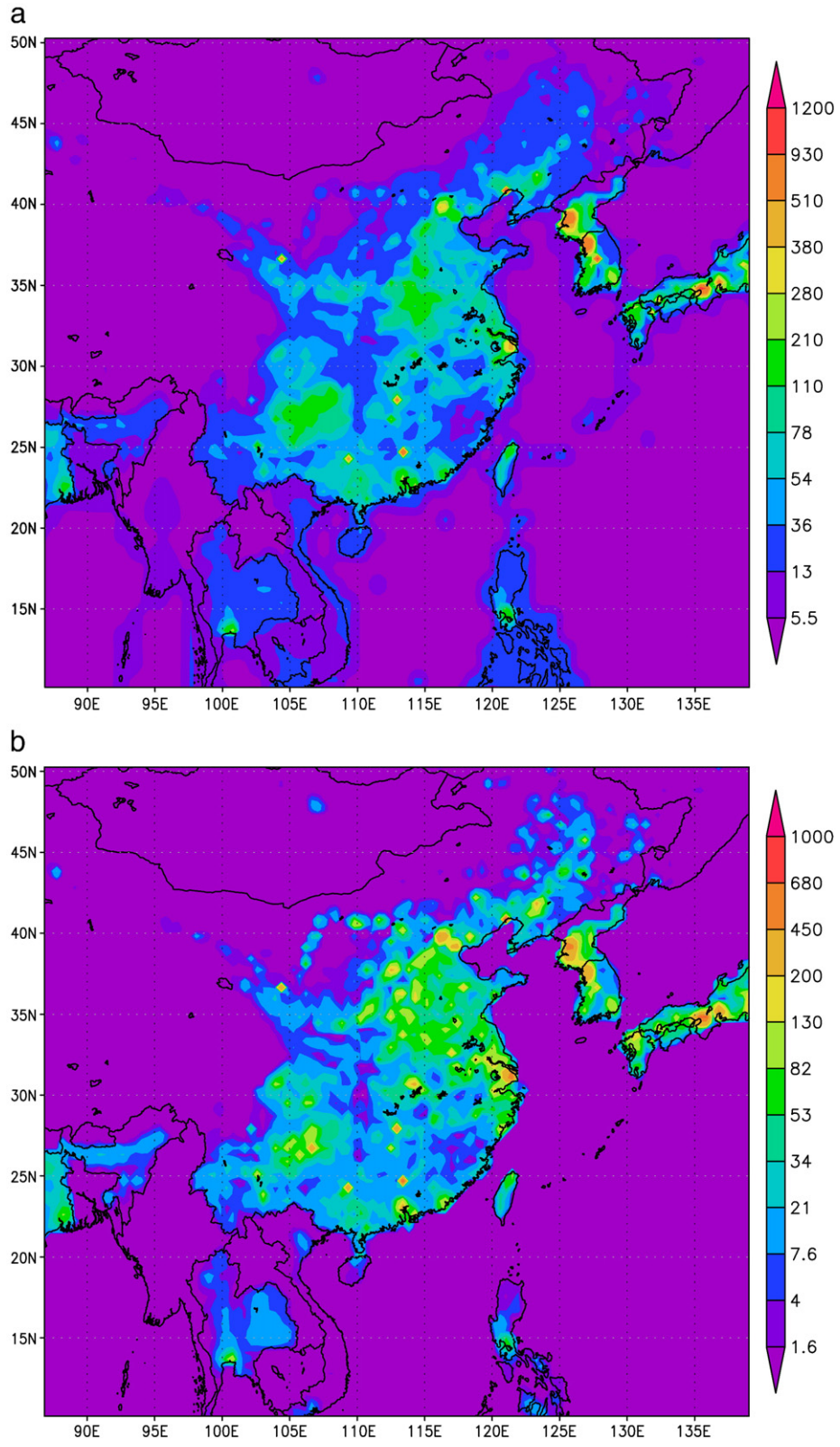

Fig. 1. The spatial distribution of mercury emission (g km^{-2} $year^{-1}$). (a) GEM, (b) RGM and (c) PHg.

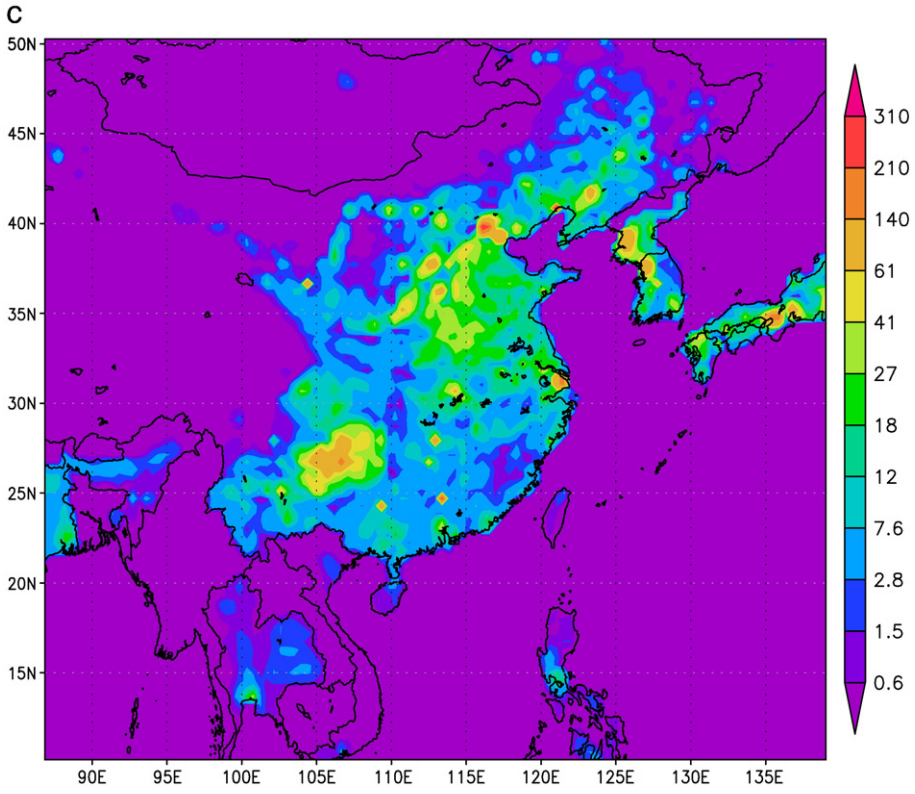

Fig. 1 (*continued*).

as the average concentration of the lowest 5% mercury concentrations measured in ACE-Asia field experiment during March and April 2001 (Friedli et al., 2004; Pan et al., 2006). The influences of IC/BCs for RGM and PHg on model results have been shown to be less significant (Pongprueksa et al., 2008). Since measured PHg concentrations in ACE-Asia field experiment were quite low (Friedli et al., 2004), zero concentration of RGM and PHg were to represent the conditions in a clean atmospheric. Two chemistry sensitivity cases, "2001_FAST" and "2001_FAST_NOEM", used the higher oxidation rate for the Hg^0–O_3 reaction (Pal and Ariya, 2004) compared to the settings in "2001_BASE" and "2001_BASE_NOEM". All simulations were spun-up for one month before simulation, which was more than sufficient for a regional domain such as the one used in this study (Pongprueksa et al., 2008). The details for the different model configurations are summarized in Table 2.

3. Results

3.1. Model verification

STEM-Hg had been previously verified by Pan et al. (2008) using observational data measured in 16 flights during ACE-Asia campaign in April 2001 (Friedli et al., 2004). In this study, the surface observations of GEM, RGM and PHg in the model domain reported over the past few years were used for model evaluation (Fang et al., 2001; Liu et al., 2002; Fang et al., 2004; Feng et al., 2004; Kim et al., 2005; Liu et al., 2005; Wang et al., 2006; Nguyen et al., 2007; Wang et al., 2007; Chand et al., 2008; Fu et al., 2008a,b,c; Kim et al., 2009; Wan et al., 2009a,b; Xiu et al., 2009; Yang et al., 2009). There were fourteen reported observations for GEM, seven observations for PHg, and four observations for RGM. Eleven of the fourteen GEM sites were located in China, two sites were in South Korea and one was in Japan. The scarcity of the observations for dry and wet mercury deposition limited the evaluation of simulated mercury deposition. The majorities of observations were made in urban areas (Beijing and Seoul) and were not measured in the same year as the modeling period. Therefore, the annual mean concentrations and the range of model results are used in the comparison. Table 3 lists the site information, observed concentrations and model predictions in the "2001_BASE" scenario.

In Table 3, model predictions under-predicted GEM and over-predicted RGM and PHg. In particular, the model-predicted GEM concentrations better in South Korea, Japan and rural areas of China, but GEM observations were underestimated by a factor 5–10 in urban

Table 2
Summary of the model scenarios in this study.

Simulations	Model configurations		
	Emissions	IC/BCs	Hg^0–O_3
2001_BASE	Anthropogenic + natural emissions	Regridded from GEOS-Chem	3.0×10^{-20} cm^3 mol^{-1} s^{-1} (Hall, 1995)
2001_BASE_NOEM	No emission	Regridded from GEOS-Chem	3.0×10^{-20} cm^3 mol^{-1} s^{-1} (Hall, 1995)
2001_CLEAN	Anthropogenic + natural emissions	GEM = 1.2 ng m^{-3} RGM/PHg = 0	3.0×10^{-20} cm^3 mol^{-1} s^{-1} (Hall, 1995)
2001_FAST	Anthropogenic + natural emissions	Regridded from GEOS-Chem	7.5×10^{-19} cm^3 mol^{-1} s^{-1} (Pal and Ariya, 2004)
2001_FAST_NOEM	No emission	Regridded from GEOS-Chem	7.5×10^{-19} cm^3 mol^{-1} s^{-1} (Pal and Ariya, 2004)

Table 3
Comparisons of model predictions in the"2001_BASE" scenarios with observations.

Station	Location	Category	Observations			Period	Model results			Ref.
			GEM(ng m^{-3})	RGM(pg m^{-3})	PHg(pg m^{-3})		GEM(ng m^{-3})	RGM(pg m^{-3})	PHg(pg m^{-3})	
Waliguan, China	100.9E 36.3N	Remote	1.7 ± 1.1			Dec-05	1.5(1.2–2.1)			1
			0.6 ± 0.1			Aug-05				
Yangze delta, China	120.7E 30.8N	Suburban	5.4 ± 4.1			Sep-05	1.8(1.0–3.6)			1
Guang Zhou, China	113.3E 23.2N	Urban	13.5 ± 7.1			Jan-05	1.7(1.2–4.1)			1
Beijing, China	116.4E 39.9N	Urban	8.3 ± 3.6		180–3510	Jan-05	1.8(1.4–2.9)		256(33–759)	1,2
			6.5 ± 5.2			Apr-05				
			4.9 ± 3.3			Jul-05				
			6.7 ± 3.5			Oct-05				
Beijing huairou, China	116. 7E 40.0N	Rural	1.8–4.6			Feb-98	1.7(1.4–2.5)			3
Chang Chun, China	125.3E 43.8N	Urban	18.4(4.7–79.6)		22–1984	Jul-09–Jul-00	1.6(1.4–3.0)		108(7–561)	4,5
		Suburban	11.7(2.3–25.6)							
Gui Yang, China	106.7E 26.6N	Urban	8.4 ± 4.9			Nov-01–Nov-02	1.8(1.3–2.2)			6
Chong Qing, China	106.5E 29.5N	Urban	6.74 ± 0.37			Aug-06–Sep-07	1.8(1.3–2.3)			7
Shanghai China	121.4E 31.1N	Urban			70–1450	Jul-04–Apr-06			180(32–581)	8
Mt_gongga, China	102.7E 29.9N	Remote	4.0(0.5–21.0)	6.2	30.7	May-05–Apr-06	1.6(1.20–2.2)	81(2.6–221)	98(9–408)	9,10
Changbaisan, China	128.3E 42.2N	Remote	3.58 ± 1.78	65.0	77.0	Aug-05–Jul-06	1.5(1.3–2.5)	39(0.3–166)	80(7–396)	11,12
Seoul, Korea	127.0E 37.5N	Urban	3.22 ± 2.1	27.2 ± 19.3	23.9 ± 19.6	Feb-05–Feb-06	2.1(1.3–3.3)	280(45–829)	173(31–5441)	13
An-myum-island, Korea	126.3E 36.5N	Rural	4.6 ± 2.2			Dec-04–Apr-06	1.7(1.3–2.8)			14
Cape-Hedo, Japan	128.2E 26.8N	Remote	2.04 ± 0.38	4.5 ± 5.4	3.0 ± 2.5	Mar-04–May-04	1.5(1.1–1.9)	39.2(0.3–174)	134(0.5–555)	15

Notes: [1]Wang et al. (2007); [2]Wang et al. (2006); [3]Liu et al. (2002); [4]Fang et al. (2004); [5]Fang et al. (2001); [6]Feng et al. (2004); [7]Yang et al. (2009); [8]Xiu et al. (2009); [9]Fu et al. (2008b); [10]Fu et al. (2008c); [11]Wan et al. (2009b); [12]Wan et al. (2009a); [13]Kim et al. (2009); [14]Nguyen et al. (2007); [15]Chand et al. (2008).

sites in China. This was mainly due to the incapability of a regional model to predict the transient peaks observed at ground levels due to the model assumption of instantaneous emission dilution in grid cells (Pongprueksa et al., 2008). Another reason might be due to the uncertainty of the emission estimates of GEM from natural sources and re-emission (Pan et al., 2006, 2007) and the mercury emission inventory that were not accounted for. For RGM and PHg concentrations, model under-predicted the observations in China but over-predicted those in Korea and Japan. The former may be due to the underestimated mercury emission; while the latter may be due to the slower removal processes of divalent mercury in Korea and Japan. Although discrepancies between predictions and observations existed to certain degree, Table 3 the model was capable of capturing the chemical transport of atmospheric mercury.

3.2. Annual mean concentrations

The annual average surface concentrations predicted by model are shown in Fig. 2. The predicted concentrations of GEM, RGM and PHg were in the ranges of 1.5–2.0 ng m^{-3}, 70–200 pg m^{-3} and 120–230 pg m^{-3}, respectively. Elevated atmospheric mercury concentrations (i.e., GEM>2.5 ng m^{-3}) were simulated in central and eastern coastal areas of China, Korea and Japan as a greater quantity of mercury emissions were reported in those areas (Fig. 1a). The simulated concentrations were comparable to global model results (Seigneur et al., 2004). For both RGM and PHg, the concentrations decreased rapidly away from anthropogenic emission sources, suggesting that RGM or PHg were readily removed away from the emission sources.

3.3. Impact of large point sources

Mercury emissions from large point sources accounted for 45% of mercury anthropogenic emissions in China (Table 1) in 2001. Most of the emissions were released from smelting processes of zinc and lead (Streets et al., 2005). There were several hot spots caused by the large point source emissions (>10 Mg $year^{-1}$), as shown in Fig. 2a, b and c. These areas had elevated GEM concentrations in the surrounding grid cells near the emission sources. In contrast to the area sources that emit mercury in the surface layer, emissions from point sources are released at higher altitudes and temperatures. As a result, they have a greater potential to enter the free troposphere and to be transported over great distances. The larger point source signals were evident in the downwind and extended to several hundred miles away. For example, the largest point source in China emitted 25 Mg of GEM in 1999 (120.75E, 40.75N) in Liaoning province (one of the most important industrial bases in China). The mercury plumes from this source was detected by C130 flights #13 and #14 on April 24 and 25 over the Yellow Sea during the ACE-Asia experiments (Friedli et al., 2004). In four episodes, an average GEM concentration of 1.5 ng m^{-3} was observed at 1000 m altitude. Both backward trajectories and model analysis had illustrated that northwestern winds carried the plume from this point source to observation points over the Yellow Sea.

3.4. Dry and wet deposition

The simulated deposition in the "2001_BASE" case is shown in Fig. 3. Measured and modeled mercury wet deposition in the northern hemisphere has been found to be about 1.5–20 μg m^{-2} $year^{-1}$ (Glass and Sorensen, 1999; Mason et al., 2000; Kamman and Engstrom, 2002; Landis and Keeler, 2002; Sakata and Marumoto, 2005; Sakata et al., 2006; Lai et al., 2007; Voudouri and Kallos, 2007; Wongberg et al., 2007; Graydon et al., 2008; Selin and Jacob, 2008; Prestbo and Gay, 2009) and dry deposition has been estimated to be of the same magnitude as wet deposition (Rea et al., 1996; Caldwell et al., 2006; Marsik et al., 2007). However, these values are lower compared to the model values since earlier measurements were made mainly in rural or remote areas in North America and Europe. Deposition in East Asia are typically higher. In China, Guo et al. (2008) reported wet deposition of 34.7 μg m^{-2} $year^{-1}$ in Wujiang River Basin, a rural area in Guizhou, in 2006. Fang et al. (2004) reported wet deposition of 152.4 μg m^{-2} $year^{-1}$ and dry deposition of 165.8 μg m^{-2} $year^{-1}$ in the urban area of Changchun from July 1999 to July 2000. Wan et al. (2009a) reported wet deposition of 8.4 μg m^{-2} $year^{-1}$ and dry deposition of 16.5–20.2 μg m^{-2} $year^{-1}$ in a remote site of Changbai Mountain from August 2005 to July 2006. Modeled wet deposition in this study averaged about 5–90 μg m^{-2} $year^{-1}$ (Fig. 3b), with 39 μg m^{-2} $year^{-1}$ in Guizhou, 11 μg m^{-2} $year^{-1}$ in Changchun and was 24.2 μg m^{-2} $year^{-1}$ in Changbai Mountain. The predicted

dry deposition averaged higher than that of wet deposition with 51 μg m^{-2} $year^{-1}$, 17 μg m^{-2} $year^{-1}$ and 54 μg m^{-2} $year^{-1}$, for Guizhou, Changchun and Changbai Mountain, respectively. Several hot spots near large point sources had dry deposition greater than 300 μg m^{-2} $year^{-1}$, but most values were in the range of 10–160 μg m^{-2} $year^{-1}$ (Fig. 3a).

The annual dry deposition and wet deposition in East Asia predicted by model in 2001 were in the range of 590–735 Mg and 482–696 Mg, respectively (Table 4). The dry deposition of RGM was the most important constituent of mercury deposition in the domain. The estimated wet deposition and dry deposition was 212 and 437 Mg $year^{-1}$ for RGM, and 270 and 154 Mg $year^{-1}$ for PHg. The wet

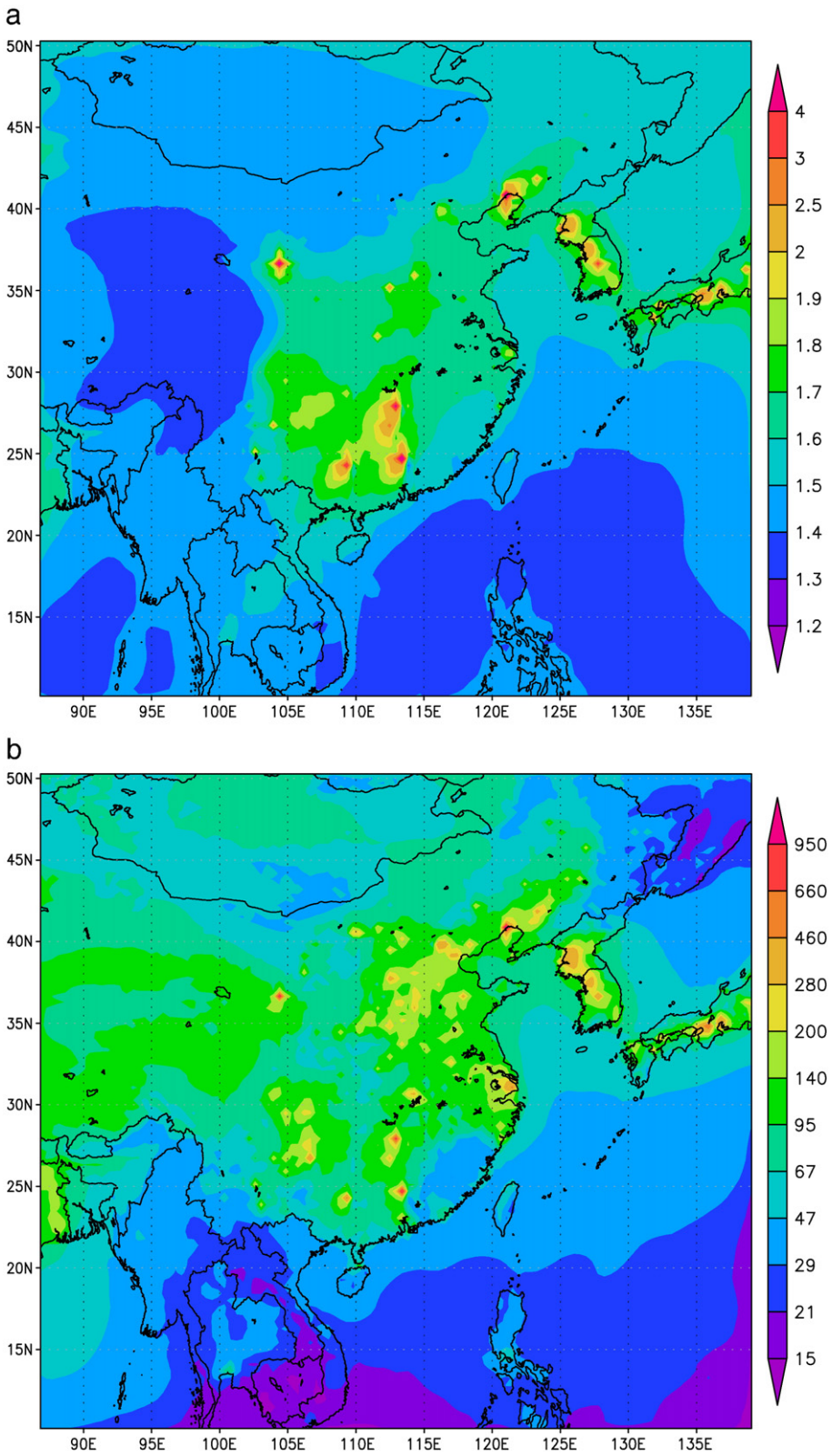

Fig. 2. Annual mean surface mercury concentration from STEM-Hg simulations under the 2001_BASE scenario. (a) GEM (ng m^{-3}), (b) RGM (pg m^{-3}) and (c) PHg (pg m^{-3}).

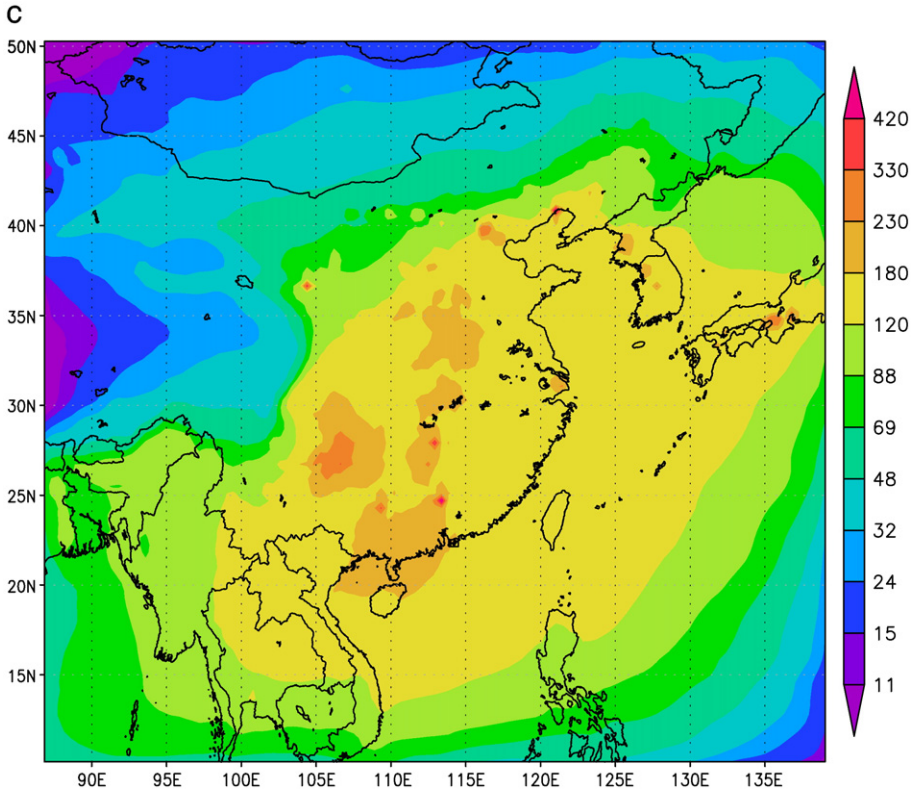

Fig. 2 (*continued*).

and dry deposition fluxes were 33.6 and 69.3 μg m^{-2} $year^{-1}$ for RGM, and 42.7 and 24.0 μg m^{-2} $year^{-1}$ for PHg. From Tables 1 and 4, the deposition of RGM and PHg was greater than their respective emissions in the domain. RGM mass entered the domain from the boundaries and sequentially deposited in the domain, which contributed 410 Mg $year^{-1}$ to the 649.1 Mg $year^{-1}$ of RGM deposition. PHg was mainly caused by the oxidation of GEM mass entering the domain from the boundaries, and contributed 325 Mg $year^{-1}$ to the 423 Mg $year^{-1}$ of PHg deposition. The direct deposition from emission also caused significant deposition. As a result, deposition was high near the source regions and gradually decreased with increasing distance away from the sources. Dry deposition and wet deposition are sensitive to mercury oxidation reactions in the gaseous phase (Lin et al., 2007). From Fig. 3a, it was also observed that dry deposition gradually decreased from land to ocean and the spatial distribution of deposition was similar to the concentration fields.

4. Discussion

4.1. Roles of emissions, boundary conditions and oxidation mechanisms

Mercury concentration and deposition in East Asia predicted by model are influenced by the within-domain emission and boundary conditions for a given simulation scenario. Among the model scenarios, the "2001_BASE_NOEM" case allowed estimating the influence of boundary conditions, while the differences in model results between the "2001_BASE" and "2001_BASE_NOEM" cases represented the contribution from the within-domain emissions. Based on the model results, the within-domain emissions contributed to 20% of total atmospheric mercury (THg) concentrations in the surface layer and 32% of total deposition (Fig. 4a and b). The month-by-month variability of mercury deposition (26–39%) is shown in Table 5. The contribution caused by the boundary conditions far exceeds those by the within-domain emission (80% to concentration and 68% to deposition). This is consistent with the earlier finding that mercury concentration and deposition in a regional domain can be significantly affected by the boundary conditions (Pongprueksa et al., 2008).

Simulated concentration and deposition are also sensitive to mercury oxidation mechanisms (Seigneur et al., 2006). The differences in simulated mercury concentration and deposition caused by the "2001_BASE" and "2001_FAST" cases are shown in Fig. 4c and d. The areas with the greatest impacts occurred in southeast China where ozone concentrations were also relatively higher. The higher oxidation kinetics caused a 9% decrease in THg concentration and a 40% increase in mercury deposition. In remote regions such as the northern region of the domain, the increase in mercury deposition was more than 100% because of the low RGM and PHg mercury emissions. Under such circumstances, oxidation of GEM is the primary cause of deposition (Lin et al., 2007).

4.2. Role of trans-boundary transport

Several long-range transport events were observed during the ACE-Asia field experiments in April 2001. Based on the ACE-Asia observations (Friedli et al., 2004), on April 11, 2001, the C130 flight #6 flew over Yellow Sea and measured GEM concentrations greater than 2.5 ng m^{-3} at altitudes above 5 km. The next C130 flight #7 on April 12, another Yellow Sea flight, observed the same signals at almost the same locations where mercury concentrations greater than 3.0 ng m^{-3} were detected at altitudes above 5 km. Backward trajectory and adjoint sensitivity analysis (Sandu et al., 2005; Pan et al., 2007) indicated that the high concentrations were likely caused by long-range transport rather than emission sources in China.

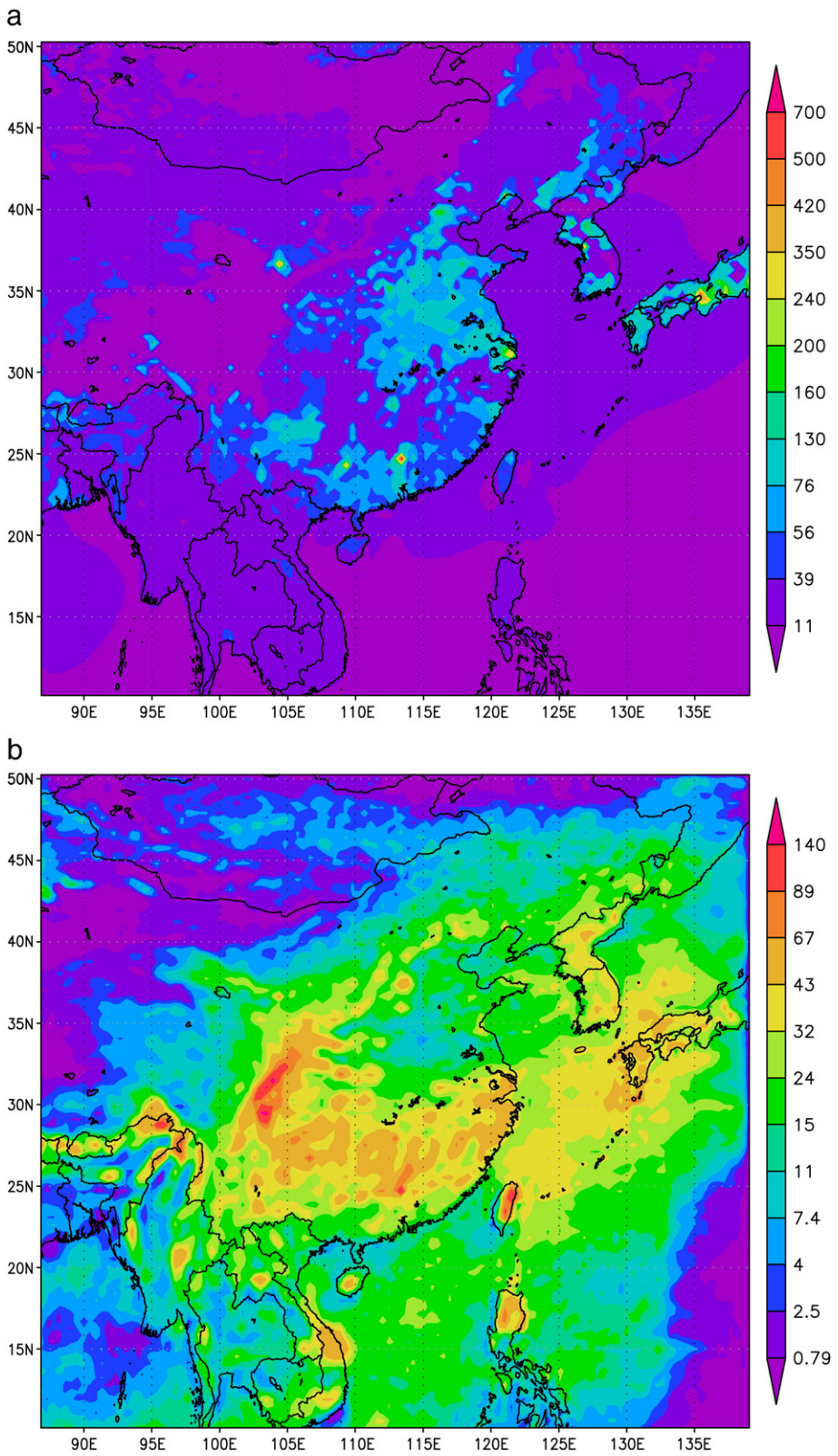

Fig. 3. Annual mean mercury deposition from STEM-Hg simulations under the 2001_BASE scenario. (a) Dry deposition (μg m^{-2} $year^{-1}$) and (b) wet deposition (μg m^{-2} $year^{-1}$).

The annual average of THg concentration in the boundary conditions employed in the "2001_BASE" case is shown in Fig. 5. The THg concentrations were typically above 1.4 ng m^{-3}. GEM concentrations in the west and north boundaries were generally above 1.7 ng m^{-3}. These were the crucial pathways of mercury plumes entering the domain from Middle Asia, India and Russia. The concentrations in the east boundary were typically greater than 1.9 ng m^{-3} as the East Asian plumes leave the model domain.

Table 4
Mass budgets of atmospheric mercury in the model domain for the model year 2001 (unit: Mg).

Species	GEM				RGM				PHg				THg			
	Slow	Slow*[a]	Fast	Fast*	Slow	Slow*	Fast	Fast*	Slow	Slow*	Fast	Fast*	Slow	Slow*	Fast	Fast*
Initial condition	307.8	294	287.2	276.1	24.3	23.2	25	23.8	6.1	4.6	19	16.9	338.2	321.8	331.2	316.8
Final condition	306.4	294.1	286.9	275.8	24.9	23.5	24.9	23.5	7.1	5.5	22.3	19.8	338.4	323.1	334.1	319.1
Emission	737.9	0.0	737.9	0.0	232.9	0.0	232.9	0.0	79	0.0	79	0.0	1049.8	0.0	1049.8	0.0
Wet deposition	0.0	0.0	0.0	0.0	212.1	139.3	220.8	146.9	269.5	209.7	474.7	386.9	481.6	349	695.5	533.8
Dry deposition	0.0	0.0	0.0	0.0	437	270.3	432.9	278.3	153.5	115.3	301.8	249.8	590.3	385.6	734.7	528.1
Net Outflow[b]	739.4		737.9		−6.9		4.2		−18.9		−61.2		713.6		680.9	

[a] * indicates the model results without mercury emission input.
[b] Based on Eq. (4).

Boundary concentrations at low altitudes (<2 km) were higher than those at high altitudes (>2 km). GEM concentration of 1.2 ng m^{-3} was considered the "background" concentration based on the observed concentrations during ACE-Asia (Pan et al., 2006). Therefore, the concentration was used for the "2001_CLEAN" case as the uniform lateral, while RGM and PHg concentrations were set to zero to assess the impact of the trans-boundary transport of mercury.

The impact of out-of-boundary mercury emissions was estimated by the differences in model results between the "2001_BASE" and "2001_CLEAN" cases. The fractional changes of THg and deposition caused by the trans-boundary transport are shown in Fig. 6a and b, respectively. The mercury trans-boundary transport, on average, enhanced the total gaseous mercury concentration and deposition by 10% and 24% in the central area and east coast of China, respectively. Travnikov (2005) studied the intercontinental transport of mercury in Northern Hemisphere and estimated that external sources did not contribute more than 32% to mercury deposition in Asia. The model estimates in this study were comparable to those by Travnikov (2005). This suggests that East Asia should not only be considered as an important source region in global mercury transport, but also a receptor region affected by other global emissions.

4.3. Mercury outflow from East Asia

Earlier studies have indicated that mercury outflow from the East Asia can have a significant influence on mercury deposition in North America (Seigneur et al., 2004). In this section, the quantity of mercury emission outflow from the region was estimated based on the regional mass budgets of atmospheric mercury. In a chemical transport model, the mass balance for mercury in the model domain can be expressed as:

$$Initial + Inflow + Emission = Final + Outflow + Deposition \quad (1)$$

where *initial* and *final* represent the total mercury masses in the model domain (Mg) at the beginning and end of the simulation period. Therefore:

$$Outflow = Initial - Final + Emission + Inflow - Deposition. \quad (2)$$

Since the mercury outflow from a regional model domain can be significantly influenced by the boundary conditions, the *outflow* term in Eq. (2) caused by boundary condition influence can be expressed as:

$$Outflow^* = Initial^* - Final^* + Inflow - Deposition^*. \quad (3)$$

The asterisk (*) represents the case in which no mercury emissions were included in the simulations. Subtracting Eq. (3) from Eq. (2), the net outflow caused by the within-domain emissions can be quantified:

$$Outflow - Outflow^* = Initial - Initial^* - Final + Final^* + Emission - Deposition + Deposition^*. \quad (4)$$

A positive value of the net outflow indicates an excess amount of mercury escaping the domain, causing long-range transport to other regions or contributing to the global mercury pool. A negative value indicates a net removal of mercury mass from air within the model domain.

Table 4 summarizes the annual mercury mass budgets in the study domain for the "2001_BASE" and "2001_FAST" scenarios. The net mercury outflow for the two scenarios (Eq. (4)), mainly in the form of GEM, was estimated to be 714 Mg and 681 Mg of THg for the year 2001, respectively. Applying Eq. (4) for the model results in the "2001_BASE" case, there was a net outflow of 739.4 Mg GEM, and a net deposition of 6.9 Mg RGM and 18.9 Mg PHg. In the "2001_FAST" case, there was a net outflow of 737.9 Mg GEM and 4.2 Mg RGM, and a net deposition of 61.2 Mg PHg. Summing up all three mercury species, using the higher Hg^0–O_3 oxidation rate (Pal and Ariya, 2004) resulted in a difference of 4.6% of the estimated net mercury outflow (from 714 to 681 Mg). The higher oxidation rate also increased RGM outflow (from −6.9 to 4.2 Mg) and PHg deposition (from 18.9 to 61.2 Mg). From Table 4, the deposition estimated by model in both "no emission" cases (i.e., deposition caused by boundary condition only) was very significant. The mercury mass from the boundary conditions contributed 735 Mg $year^{-1}$ to the 1072 Mg $year^{-1}$ of total deposition in the "2001_BASE" case; and 1062 Mg $year^{-1}$ to the 1430 Mg $year^{-1}$ of total deposition in "2001_FAST" case. Overall, we estimated that 70% of mercury emissions ended up becoming mercury mass outflow, compared to the 75% reported by Lin et al. (2010) using CMAQ-Hg.

4.4. Seasonal trend of mercury cycling in the domain

Based on the model results in the "2001_BASE" scenario, both mercury concentration and deposition showed strong seasonal variation (Table 5). The domain-averaged GEM surface concentrations were higher in winter and spring, and lower in summer and fall. This was in agreement with the seasonal trend observed in China (Feng et al., 2004; Wang et al., 2007; Fu et al., 2008a). PHg concentrations were higher in summer and peaked in August because of the higher photochemical activities. RGM concentrations did not show a clear trend as those for GEM and PHg, but was higher in late winter and early spring due to the lower mixing heights. Deposition was greater in summer and fall due to the higher concentration of PHg, as well as greater dry deposition velocities of mercury species and precipitation in both seasons.

The impacts of within-domain emissions and boundary conditions on mercury concentration and deposition were also shown in Table 5, which were calculated using the model results of "2001_BASE" and "2001_BASE_NOEM" cases. Transport of mercury from the boundaries contributed 68% of the total mercury deposition in the domain compared to the 32% caused by within-domain emissions. The results

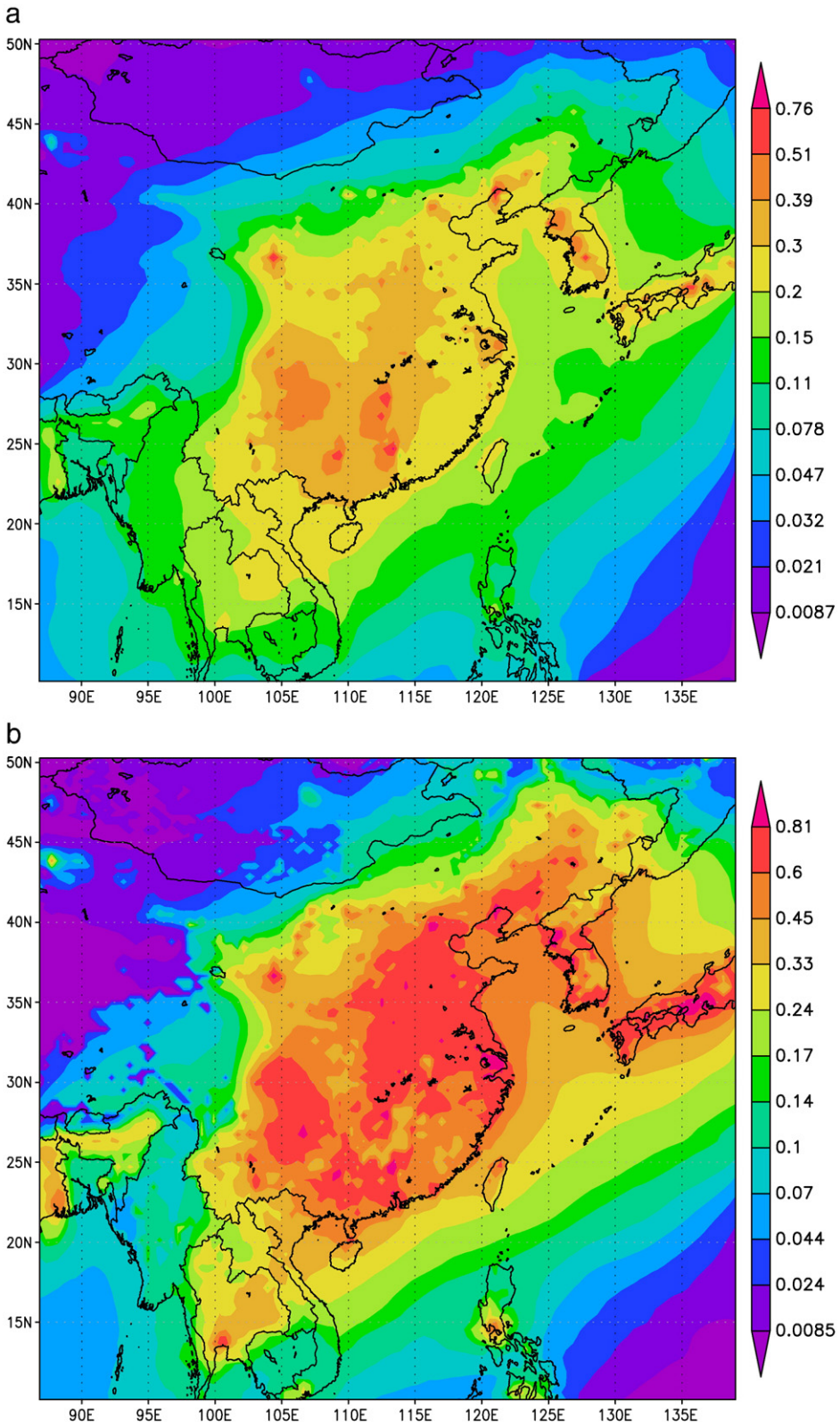

Fig. 4. Effects of domain emissions and chemical mechanisms on mercury surface concentration and deposition: (a) fraction of THg concentration contributed by domain emissions, (b) fraction of total deposition contributed by domain emissions, (c) ratio of THg concentration in the "2001_FAST" case over that in the "2001_BASE" case, and (d) ratio of total deposition in the "2001_FAST" case over that in the "2001_BASE" case.

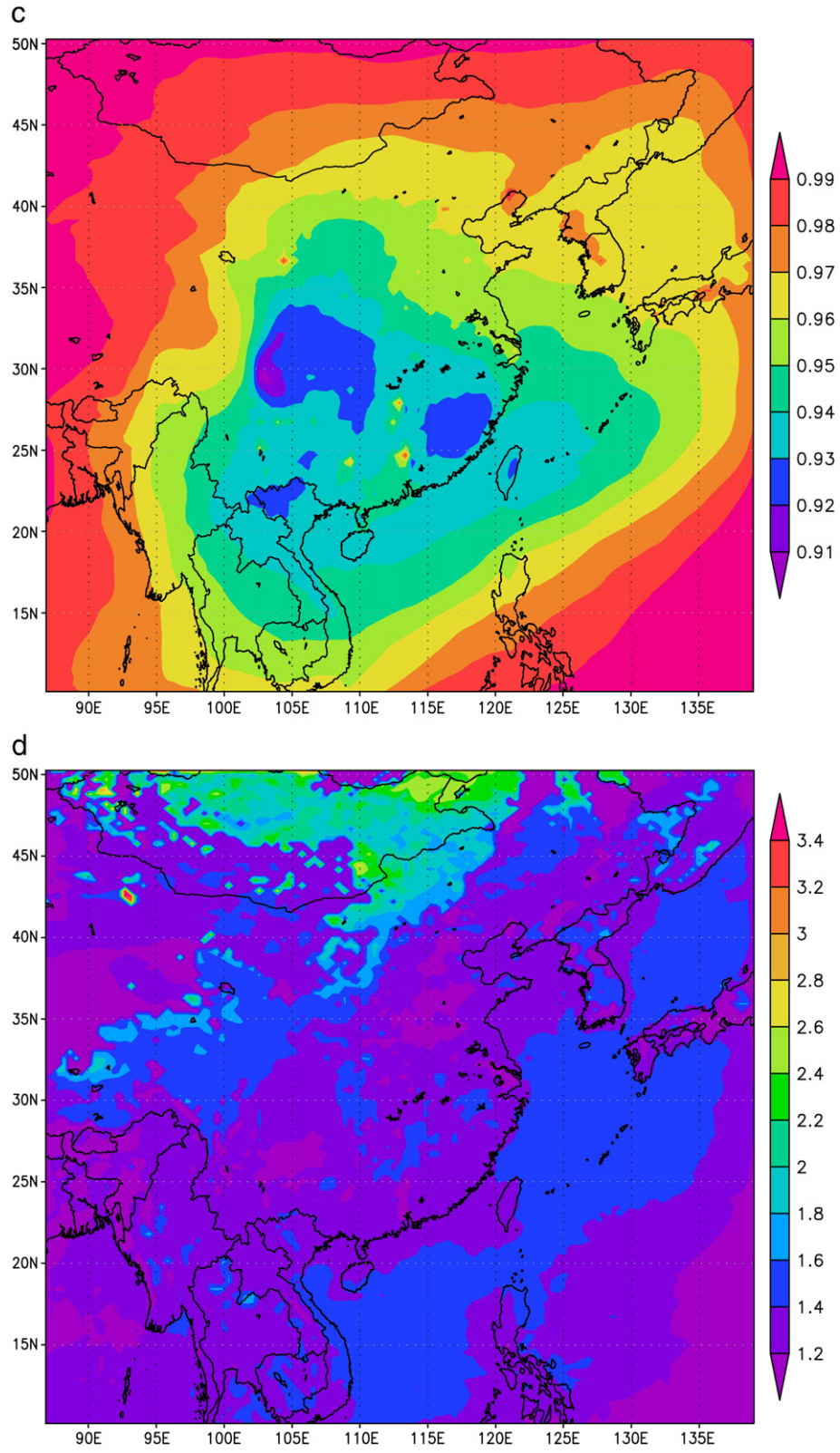

Fig. 4 (*continued*).

indicated that boundary conditions were the most important contributing factors controlling the mercury seasonal cycle in a regional domain. The deposition caused by the boundary conditions was relatively constant, ranging from 61 to 74% (Table 5).

It is important to note that the net outflow caused by mercury emissions released in the domain is independent of boundary conditions based on the methodology in this study (Lin et al., 2010). Greater outflows were estimated in spring and early summer, with

Table 5
Monthly variations of Hg emission, concentration, deposition, mass outflow and emission contribution to deposition.

Items	Month											
	Jan	Feb	Mar	Apr	May	Jun	Jul	Aug	Sep	Oct	Nov	Dec
Natural emission (Mg)	10.6	11.9	17.2	25.1	35.7	41.0	43.6	39.8	31.7	19.8	14.4	13.2
Biomass emission (Mg)	0.7	1.2	10.1	15.2	0.1	0.04	0.03	0.04	0.06	0.17	0.04	0.04
GEM at surface (ng m^{-3})	1.52	1.50	1.51	1.50	1.47	1.46	1.46	1.50	1.48	1.51	1.51	1.53
RGM at surface (pg m^{-3})	64.5	69.8	72.9	66.6	59.7	53.1	50.2	53.8	55.5	64.2	74.0	58.6
PHg at surface (pg m^{-3})	45.9	50.2	61.3	80.7	95.3	111.7	127.7	148.2	129.0	97.8	67.3	48.5
Deposition (Mg $month^{-1}$)	80.8	78.8	85.5	93.6	101.5	100.3	99.6	103.8	101.5	86.7	68	71.8
Deposition caused by within-domain emission* (%)	32	29	39	26	27	30	30	30	33	35	35	34
Deposition caused by boundary conditions** (%)	68	71	61	74	73	70	70	70	67	65	65	66
Hg outflow (Mg $month^{-1}$)	48.7	44.7	54.3	71.1	70.1	68.5	68.2	60.3	61.2	55.3	58.1	53

Note:

- *. $\frac{1-2001\_BASE\_NOEM}{2001\_BASE \times 100\%}$
- **. $\frac{2001\_BASE\_NOEM}{2001\_BASE \times 100\%}$

April having the maximum outflow (Table 5). In winter and fall, the outflows were smaller, due to lower natural emissions (Shetty et al., 2008).

5. Conclusions

The STEM-Hg model was employed to simulate the transport, transformation and deposition of mercury in East Asia in 2001. The model results provided insights to the annual cycling and its seasonal variability of atmospheric mercury and agreed reasonably with the limited observations made in the region. Model-predicted annual mean concentrations of GEM, RGM and PHg in the eastern and central China, Korea and Japan were 1.8 ng m^{-3}, 100 pg m^{-3} and 150 pg m^{-3}, respectively. Ambient GEM concentration exhibited seasonal variation with higher concentrations in winter and spring. PHg concentrations were higher in summer while RGM concentrations did not show a clear trend.

Strong signals from large point sources strongly influenced the simulated mercury concentrations and deposition at both local and regional scales. Model-predicted deposition in the region is 2–3 times greater than the measurements reported in North America and Europe. The estimated annual dry deposition and wet deposition in the domain were in the ranges of 590–735 Mg and 482–696 Mg, respectively. Mercury deposition was greater in the summer and fall.

Boundary conditions played a dominant role based on our simulation results, indicating the importance of trans-boundary transport of mercury. The boundary conditions contributed to about 80% of mean surface concentration and about 70% of total deposition, compared to the 20% and 30% caused by the within-domain emissions. Mercury mass inflows above the "clean" background (i.e., >1.2 ng m^{-3} GEM) increased mercury concentration by 10% and deposition by 24% in the domain, suggesting the impact of out-of-boundary emissions. Changing Hg^0–O_3 reaction rate to the higher value forced a 9% decrease of mercury concentration and a 40% increase in mercury deposition.

The regional mass budgets of atmospheric mercury were estimated to quantify mercury emission outflow from the East Asian region. The net mercury outflows showed strong seasonal variation and totaled 714 Mg $year^{-1}$ (predominantly GEM), but

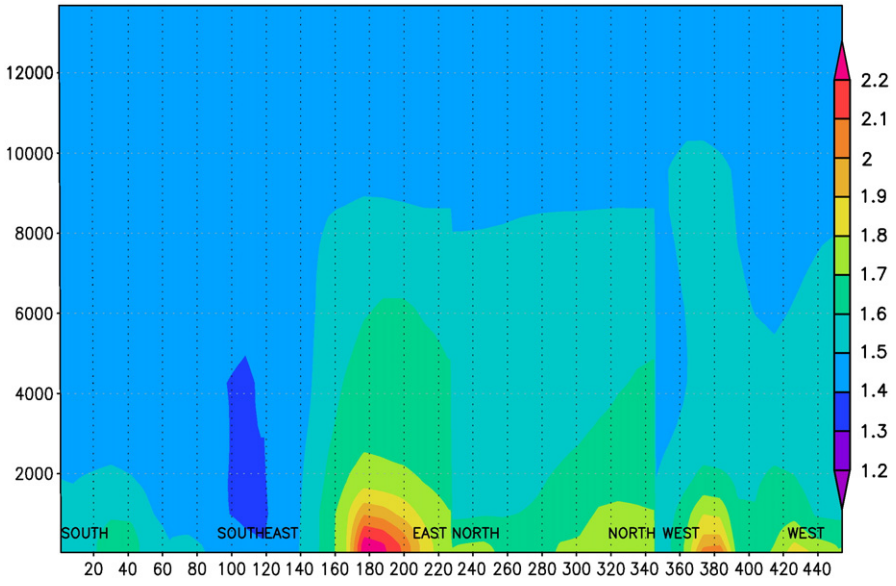

Fig. 5. Annual mean concentration of THg (ng m^{-3}) in the boundary conditions of the 2001_BASE scenario.

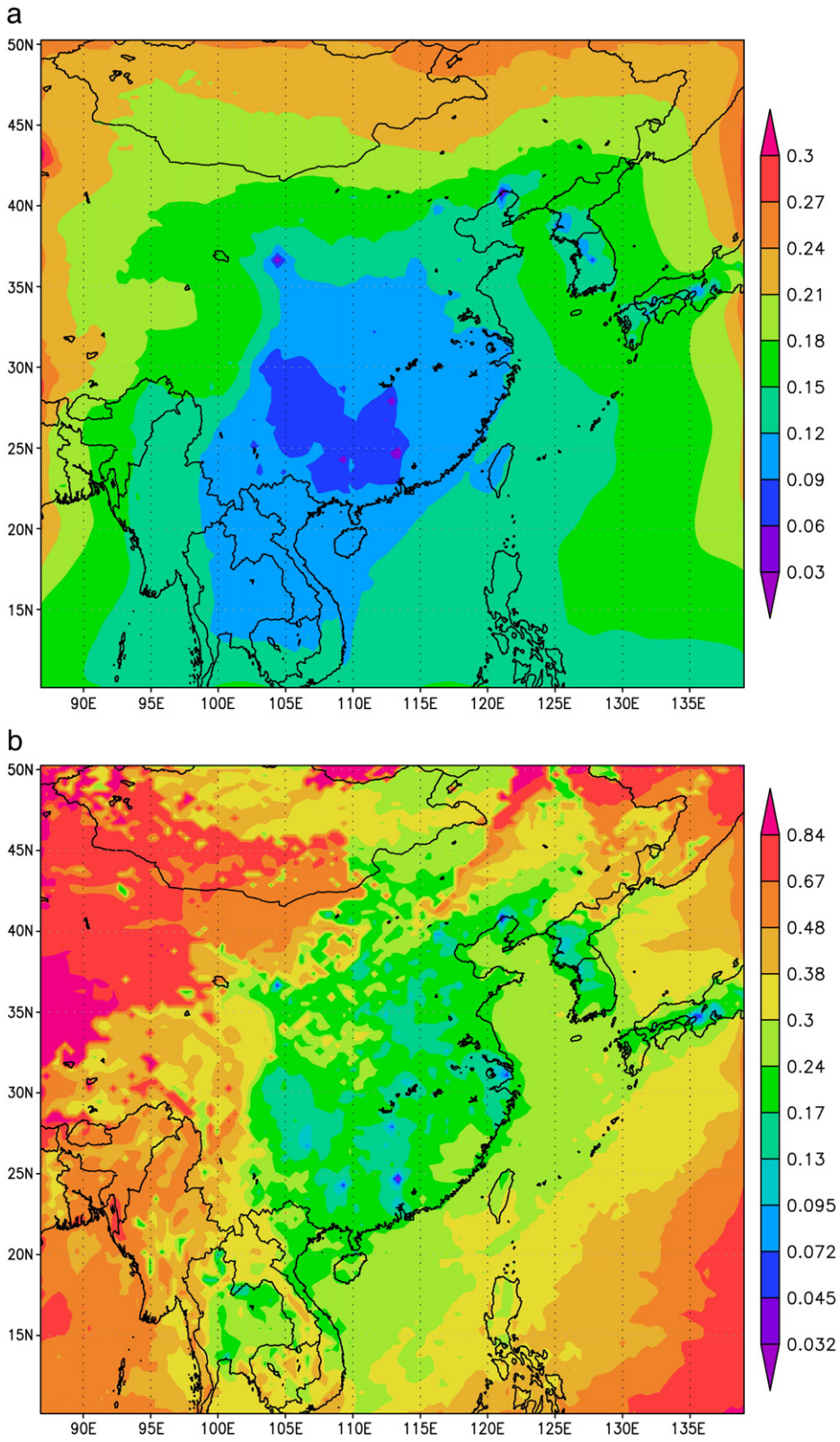

Fig. 6. Fractional changes of (a) THg concentration and (b) total deposition caused by the mercury concentrations above the "background" concentration (GEM of 1.2 ng m^{-3}) The fractional changes were calculated from the model results of the "2001_BASE" and the "2001_CLEAN" cases. The case description is shown in Table 2.

reduced to 681 Mg $year^{-1}$ when a faster (Hg^0–O_3) oxidation rate was employed. The strongest mercury outflows occurred in spring followed by May and February in the modeling year based on the model results.

Acknowledgements

The study is sponsored in parts by the USEPA through a subcontract from EC/R (Contract No.: PO1-OPR402-LAM), Texas Air Research Center

(Project No: 078LUB3068A), Texas Commission on Environmental Quality (2005–2009 Umbrella Contract No. 582-7-83975) and the State Key Laboratory of Environmental Geochemistry, Institute of Geochemistry, Chinese Academy of Sciences. The funding support is gratefully acknowledged.

References

Bullock OR, Brehme KA. Atmospheric mercury simulation using the CMAQ model: formulation description and analysis of wet deposition results. Atmos Environ 2002;36(13):2135–46.
Caldwell CA, Swartzendruber P, Prestbo E. Concentration and dry deposition of mercury species in arid south central New Mexico (2001–2002). Environ Sci Technol 2006;40(24):7535–40.
Calori G, Carmichael GR. An urban trajectory model for sulfur in Asian megacities: model concepts and preliminary application. Atmos Environ 1999;33(19): 3109–17.
Carmichael GR, Peters LK, Kitada T. A 2nd generation model for regional-scale transport chemistry deposition. Atmos Environ 1986;20(1):173–88.
Carmichael GR, Peters LK, Saylor RD. The STEM-II regional scale acid deposition and photochemical oxidant model—I. An overview of model development and applications. Atmos Environ Part A Gen Top 1991;25(10):2077–90.
Carmichael GR, Uno I, Phadnis MJ, Zhang Y, Sunwoo Y. Tropospheric ozone production and transport in the springtime in east Asia. J Geophys Res Atmos 1998;103(D9): 10649–71.
Carmichael GR, Tang Y, Kurata G, Uno I, Streets D, Woo JH, et al. Regional-scale chemical transport modeling in support of the analysis of observations obtained during the TRACE-P experiment. J Geophys Res Atmos 2003;108(D21) GTE 44/1-GTE 44/28.
Carter WPL. Implementation of the SAPRC-99 chemical mechanism into the models-3 framework; 2000.
Chand D, Jaffe D, Prestbo E, Swartzendruber PC, Hafner W, Weiss-Penzias P, et al. Reactive and particulate mercury in the Asian marine boundary layer. Atmos Environ 2008;42(34):7988–96.
Cohen M, Artz R, Draxler R, Miller P, Poissant L, Niemi D, et al. Modeling the atmospheric transport and deposition of mercury to the Great Lakes. Environ Res 2004;95(3):247–65.
Fang F, Wang Q, Liu R, Ma Z, Hao Q. Atmospheric particulate mercury in Changchun City, China. Atmos Environ 2001;35(25):4265–72.
Fang FM, Wang QC, Li JF. Urban environmental mercury in Changchun, a metropolitan city in Northeastern China: source, cycle, and fate. Sci Total Environ 2004;330(1–3): 159–70.
Feng XB, Shang LH, Wang SF, Tang SL, Zheng W. Temporal variation of total gaseous mercury in the air of Guiyang, China. J Geophys Res Atmos 2004;109:D03303.
Friedli HR, Radke LF, Prescott R, Li P, Woo JH, Carmichael GR. Mercury in the atmosphere around Japan, Korea, and China as observed during the 2001 ACE-Asia field campaign: measurements, distributions, sources, and implications. J Geophys Res Atmos 2004;109:D19S25.
Fu X, Feng X, Zhu W, Wang S, Lu J. Total gaseous mercury concentrations in ambient air in the eastern slope of Mt. Gongga, South-Eastern fringe of the Tibetan plateau, China. Atmos Environ 2008a;42(5):970–9.
Fu XW, Feng XB, Zhu WZ, Wang SF, Lu JL. Total gaseous mercury concentrations in ambient air in the eastern slope of Mt. Gongga, South-Eastern fringe of the Tibetan plateau, China. Atmos Environ 2008b;42(5):970–9.
Fu XW, Feng XB, Zhu WZ, Zheng W, Wang SF, Lu JY. Total particulate and reactive gaseous mercury in ambient air on the eastern slope of the Mt. Gongga area, China. Appl Geochem 2008c;23(3):408–18.
Gbor PK, Wen DY, Meng F, Yang FQ, Sloan JJ. Modeling of mercury emission, transport and deposition in North America. Atmos Environ 2007;41(6):1135–49.
Glass GE, Sorensen JA. Six-year trend (1990–1995) of wet mercury deposition in the Upper Midwest, U.S.A.. Environ Sci Technol 1999;33(19):3303–12.
Graydon JA, Louis VLS, Hintelmann H, Lindberg SE, Sandilands KA, Rudd JWM, et al. Long-term wet and dry deposition of total and methyl mercury in the remote boreal ecoregion of Canada. Environ Sci Technol 2008;42(22):8345–51.
Grell G. A description of the fifth generation Penn State/NCAR mesoscale model (mm5). Cent Atmos Res Colo 1995;107.
Guo Y, Feng X, Li Z, He T, Yan H, Meng B, et al. Distribution and wet deposition fluxes of total and methyl mercury in Wujiang River Basin, Guizhou, China. Atmos Environ 2008;42(30):7096–103.
Hall B. The gas phase oxidation of elemental mercury by ozone. Water Air Soil Pollut 1995;80(1–4):301–15.
Kamman NC, Engstrom DR. Historical and present fluxes of mercury to Vermont and New Hampshire lakes inferred from 210Pb dated sediment cores. Atmos Environ 2002;36(10):1599–609.
Kim KH, Ebinghaus R, Schroeder WH, Blanchard P, Kock HH, Steffen A, et al. Atmospheric mercury concentrations from several observatory sites in the northern hemisphere. J Atmos Chem 2005;50(1):1-24.
Kim SH, Han YJ, Holsen TM, Yi SM. Characteristics of atmospheric speciated mercury concentrations (TGM, Hg(II) and Hg(p)) in Seoul, Korea. Atmos Environ 2009;43 (20):3267–74.
Lai S-O, Holsen TM, Hopke PK, Liu P. Wet deposition of mercury at a New York state rural site: concentrations, fluxes, and source areas. Atmos Environ 2007;41(21):4337–48.
Landis MS, Keeler GJ. Atmospheric mercury deposition to Lake Michigan during the Lake Michigan Mass Balance Study. Environ Sci Technol 2002;36(21):4518–24.
Lin C-J, Pehkonen SO. The chemistry of atmospheric mercury: a review. Atmos Environ 1999;33(13):2067–79.
Lin C-J, Pongprueksa P, Russell Bullock Jr O, Lindberg SE, Pehkonen SO, Jang C, et al. Scientific uncertainties in atmospheric mercury models II: sensitivity analysis in the CONUS domain. Atmos Environ 2007;41(31):6544–60.
Lin C-J, Pan L, Streets DG, Shetty S, Jang C, Feng X, et al. Estimating mercury emission outflow from East Asia using CMAQ-Hg. Atmos Chem Phys 2010;10(4):1853–64.
Liu SL, Nadim F, Perkins C, Carley RJ, Hoag GE, Lin YH, et al. Atmospheric mercury monitoring survey in Beijing, China. Chemosphere 2002;48(1):97-107.
Liu GLL, Jin QX, Zhang DN, Shi SY, Huang XJ, Zhang WY, et al. Characterization of size-fractionated particulate mercury in Shanghai ambient air. Atmos Environ 2005;39 (3):419–27.
Marsik FJ, Keeler GJ, Landis MS. The dry-deposition of speciated mercury to the Florida Everglades: measurements and modeling. Atmos Environ 2007;41(1):136–49.
Mason RP, Lawson NM, Sheu GR. Annual and seasonal trends in mercury deposition in Maryland. Atmos Environ 2000;34(11):1691–701.
Nguyen HT, Kim KH, Kim MY, Hong SM, Youn YH, Shon ZH, et al. Monitoring of atmospheric mercury at a global atmospheric watch (GAW) site on An-Myun Island, Korea. Water Air Soil Pollut 2007;185(1–4):149–64.
Pacyna EG, Pacyna JM, Steenhuisen F, Wilson S. Global anthropogenic mercury emission inventory for 2000. Atmos Environ 2006;40(22):4048–63.
Pal B, Ariya PA. Studies of ozone initiated reactions of gaseous mercury: kinetics, product studies, and atmospheric implications. Phys Chem Chem Phys 2004;6(3):572–9.
Pan L, Carmichael GR. A two-phase box model to study mercury atmospheric mechanisms. Environ Chem 2005;2(3):205–14.
Pan L, Woo JH, Carmichael GR, Tang YH, Friedli HR, Radke LF. Regional distribution and emissions of mercury in east Asia: a modeling analysis of Asian Pacific Regional Aerosol Characterization Experiment (ACE-Asia) observations. J Geophys Res Atmos 2006;111:D07109.
Pan L, Chai TF, Carmichael GR, Tang YH, Streets D, Woo JH, et al. Top–down estimate of mercury emissions in China using four-dimensional variational data assimilation. Atmos Environ 2007;41(13):2804–19.
Pan L, Carmichael GR, Adhikary B, Tang Y, Streets D, Woo J-H, et al. A regional analysis of the fate and transport of mercury in East Asia and an assessment of major uncertainties. Atmos Environ 2008;42(6):1144–59.
Pongprueksa P, Lin C-J, Lindberg SE, Jang C, Braverman T, Russell Bullock Jr O, et al. Scientific uncertainties in atmospheric mercury models III: boundary and initial conditions, model grid resolution, and Hg(II) reduction mechanism. Atmos Environ 2008;42(8):1828–45.
Prestbo EM, Gay DA. Wet deposition of mercury in the US and Canada, 1996–2005: results and analysis of the NADP mercury deposition network (MDN). Atmos Environ 2009;43(27):4223–33.
Rea AW, Keeler GJ, Scherbatskoy T. The deposition of mercury in throughfall and litterfall in the lake champlain watershed: a short-term study. Atmos Environ 1996;30(19):3257–63.
Reddy MS, Boucher O. A study of the global cycle of carbonaceous aerosols in the LMDZT general circulation model. J Geophys Res Atmos 2004;109(D14).
Rolfhus KR, Sakamoto HE, Cleckner LB, Stoor RW, Babiarz CL, Back RC, et al. Distribution and fluxes of total and methylmercury in Lake Superior. Environ Sci Technol 2003;37(5):865–72.
Sakata M, Marumoto K. Formation of atmospheric particulate mercury in the Tokyo metropolitan area. Atmos Environ 2002;36(2):239–46.
Sakata M, Marumoto K. Wet and dry deposition fluxes of mercury in Japan. Atmos Environ 2005;39(17):3139–46.
Sakata M, Marumoto K, Narukawa M, Asakura K. Regional variations in wet and dry deposition fluxes of trace elements in Japan. Atmos Environ 2006;40(3):521–31.
Sandu A, Daescu DN, Carmichael GR, Chai TF. Adjoint sensitivity analysis of regional air quality models. J Comput Phys 2005;204(1):222–52.
Seigneur C, Vijayaraghavan K, Lohman K, Karamchandani P, Scott C. Global source attribution for mercury deposition in the United States. Environ Sci Technol 2004;38(2):555–69.
Seigneur C, Vijayaraghavan K, Lohman K. Atmospheric mercury chemistry: sensitivity of global model simulations to chemical reactions. J Geophys Res Atmos 2006;111(D22).
Selin NE, Jacob DJ. Seasonal and spatial patterns of mercury wet deposition in the United States: constraints on the contribution from North American anthropogenic sources. Atmos Environ 2008;42(21):5193–204.
Selin NE, Jacob DJ, Park RJ, Yantosca RM, Strode S, Jaegle L, et al. Chemical cycling and deposition of atmospheric mercury: global constraints from observations. J Geophys Res Atmos 2007;112:D02308.
Shetty SK, Lin C-J, Streets DG, Jang C. Model estimate of mercury emission from natural sources in East Asia. Atmos Environ 2008;42(37):8674–85.
Slemr F, Schuster G, Seiler W. Distribution, speciation, and budget of atmospheric mercury. J Atmos Chem 1985;3(4):407–34.
Streets DG, Hao JM, Wu Y, Jiang JK, Chan M, Tian HZ, et al. Anthropogenic mercury emissions in China. Atmos Environ 2005;39(40):7789–806.
Strode SA, Jaegle L, Jaffe DA, Swartzendruber PC, Selin NE, Holmes C, et al. Trans-Pacific transport of mercury. J Geophys Res Atmos 2008;113:D15305.
Tang YH, Carmichael GR, Uno I, Woo JH, Kurata G, Lefer B, et al. Impacts of aerosols and clouds on photolysis frequencies and photochemistry during TRACE-P: 2. Three-dimensional study using a regional chemical transport model. J Geophys Res Atmos 2003;108(D21).
Travnikov O. Contribution of the intercontinental atmospheric transport to mercury pollution in the Northern Hemisphere. Atmos Environ 2005;39(39):7541–8.
Voudouri A, Kallos G. Validation of the integrated RAMS-Hg modelling system using wet deposition observations for eastern North America. Atmos Environ 2007;41 (27):5732–45.

Wan Q, Feng XB, Lu J, Zheng W, Song XJ, Li P, et al. Atmospheric mercury in Changbai Mountain area, northeastern China II. The distribution of reactive gaseous mercury and particulate mercury and mercury deposition fluxes. Environ Res 2009a;109(6):721–7.
Wan Q, Feng XB, Lu JL, Zheng W, Song XJ, Han SJ, et al. Atmospheric mercury in Changbai Mountain area, northeastern China I. The seasonal distribution pattern of total gaseous mercury and its potential sources. Environ Res 2009b;109(3):201–6.
Wang ZW, Zhang XS, Chen ZS, Zhang Y. Mercury concentrations in size-fractionated airborne particles at urban and suburban sites in Beijing, China. Atmos Environ 2006;40(12):2194–201.
Wang ZW, Chen ZS, Duan N, Zhang XS. Gaseous elemental mercury concentration in atmosphere at urban and remote sites in China. J Environ Sci China 2007;19(2): 176–80.
Wesely ML. Parameterization of surface resistances to gaseous dry deposition in regional-scale numerical-models. Atmos Environ 1989;23(6):1293–304.
Wongberg I, Munthe J, Berg T, Ebinghaus R, Kock HH, Temme C, et al. Trends in air concentration and deposition of mercury in the coastal environment of the North Sea area. Atmos Environ 2007;41(12):2612–9.
Wu Y, Wang SX, Streets DG, Hao JM, Chan M, Jiang JK. Trends in anthropogenic mercury emissions in China from 1995 to 2003. Environ Sci Technol 2006;40(17):5312–8.
Xiu GL, Cai J, Zhang WY, Zhang DN, Bueler A, Lee SC, et al. Speciated mercury in size-fractionated particles in Shanghai ambient air. Atmos Environ 2009;43(19): 3145–54.
Yang YK, Chen H, Wang DY. Spatial and temporal distribution of gaseous elemental mercury in Chongqing, China. Environ Monit Assess 2009;156(1–4):479–89.